Supporting Information for

Second Harmonic Generation-based Nonlinear Plasmonic RI-Sensing in Solution: Pivotal Role of Particle Size

Mrigank Singh Verma[a] *and Manabendra Chandra*[a]*

[a]Department of Chemistry, Indian Institute of Technology, Kanpur, Uttar Pradesh – 208016, India.

***Corresponding author**

Email: mchandra@iitk.ac.in

Table of contents

1. Synthesis of gold nanorods…….....S2.
2. Dimensional parameters of gold nanorods ……..……...S3.
3. Sample preparation protocol for surrounding refractive index (RI) modulation ……...……..……..……...S5.
4. Variation of LSPR maxima as a function of surrounding RI……..... S5.
5. Second-harmonic light scattering (SHLS) experiments……..…....S6.
6. Three-dimensional numerical simulations……...…S7.
7. Nonlinear plasmonic refractive index sensitivity of NR5……...….S9.
8. References……...…….S10.

1. Synthesis of gold nanorods

I. Synthesis of NR1: NR1 was synthesized by following a previously reported protocol by Chang and Murphy [S1]. It is a two-step process that involves-

I(a) Preparation of seed solution: For the first step, we synthesized very small gold nanoparticle precursors, called seeds. 0.375mL (0.01M) Au^{3+} is added to 14.625 mL of aqueous solution of CTAB (0.10M) with constant stirring. The resulting mixture turned yellow. To this mixture, 0.900 mL of ice-cold aqueous $NaBH_4$ (0.01M) is added, which turns the solution yellow-brown. The mixture is stirred vigorously for an additional 2 min, and afterward, it is kept in the dark at 27^0 C for 2 hours.

I(b) Preparation of growth solution: In the next step, 1 mL of Au^{3+} (0.01M) is added to 16 mL of aqueous solution of CTAB (0.1M) followed by an addition of 0.160 mL of Ag^+ (0.01M). To this mixture, 0.400 mL of HCl (1M) is added. 0.160 mL of Ascorbic Acid (0.1M) is added as a mild reducing agent, and finally, 4 mL of seed solution is added to initiate the growth process. The resulting growth solution is kept at 27^0C for 20 hours. It should be noted that after each addition, the tube is gently inverted for proper mixing of the reagents.

II. Synthesis of NR2: NR2 is synthesized using a seed-mediated procedure developed by Nikoobakht and El-Sayed[S2]. This again involves two steps. The first step is the preparation of a seed solution (same as for the NR1), which is used in the following step to initiate the growth of gold nanorods.

To prepare the growth solutions for NR2, 15ml of 0.20M CTAB solution is mixed with 15 ml of 1 mM Au^{3+}. To this mixture 0.600 mL of 4mM Ag^+ is added at 25^0C. In the following step, 0.210 mL of 0.0788M of Ascorbic acid is added as the reducing agent. Finally, to start the growth process, the resulting reaction mixture is added with 0.036 mL of the seed solution prepared in I(a). The final growth solution is kept at 30^0C overnight.

III. Synthesis of NR3, NR4, and NR5: For the synthesis of NR3 and NR4, we followed a one-pot synthesis procedure reported by Zhang *et al.*[S3] Here, phenol (hydroquinone) is used as a mild reducing agent instead of ascorbic acid, and the reaction is initiated with the addition of $NaBH_4$.

III(a) Synthesis of NR3: 0.912 mL of 0.01M Au^{3+} and 0.135 mL of 0.02M Ag^+ is added to 21.375 mL of 0.1M CTAB, sequentially. The mixture is gently shaken, and 0.138 mL of 0.87M aqueous solution of hydroquinone is added. After mixing it, the solution is left to stand for 5 minutes, followed by the addition of 0.078 mL of 0.5mM $NaBH_4$ to initiate the reaction.

III(b) Synthesis of NR4: Amounts of CTAB, Au^{3+}, and hydroquinone remain unaltered. In the CTAB-Au^{3+} mixture, 0.144 mL of 0.02M Ag^+ and 0.138 mL of 0.87 hydroquinone is added. The mixture is

left undisturbed for 5 minutes, and finally, 0.072 mL of 0.5mM $NaBH_4$ is added to start the growth process.

III(c) Synthesis of NR5: The synthesis procedure of NR5 remains the same as that of NR3 and NR4, apart from two changes. 0.138mL of 0.02M Ag^+ and 0.050 mL of 5mM $NaBH_4$ is added in the growth mixture of NR5.

All the growth solutions were left undisturbed at 30^0 C for 12 hrs.

All the prepared nanorods are centrifuged at 10000 RPM for 15 minutes and redispersed in HPLC water.

2. Dimensional parameters of gold nanorods (NR1-NR4)

The following figures depict the dimensional distribution of lengths, diameters, aspect ratios, and surface areas of all the nanorods.

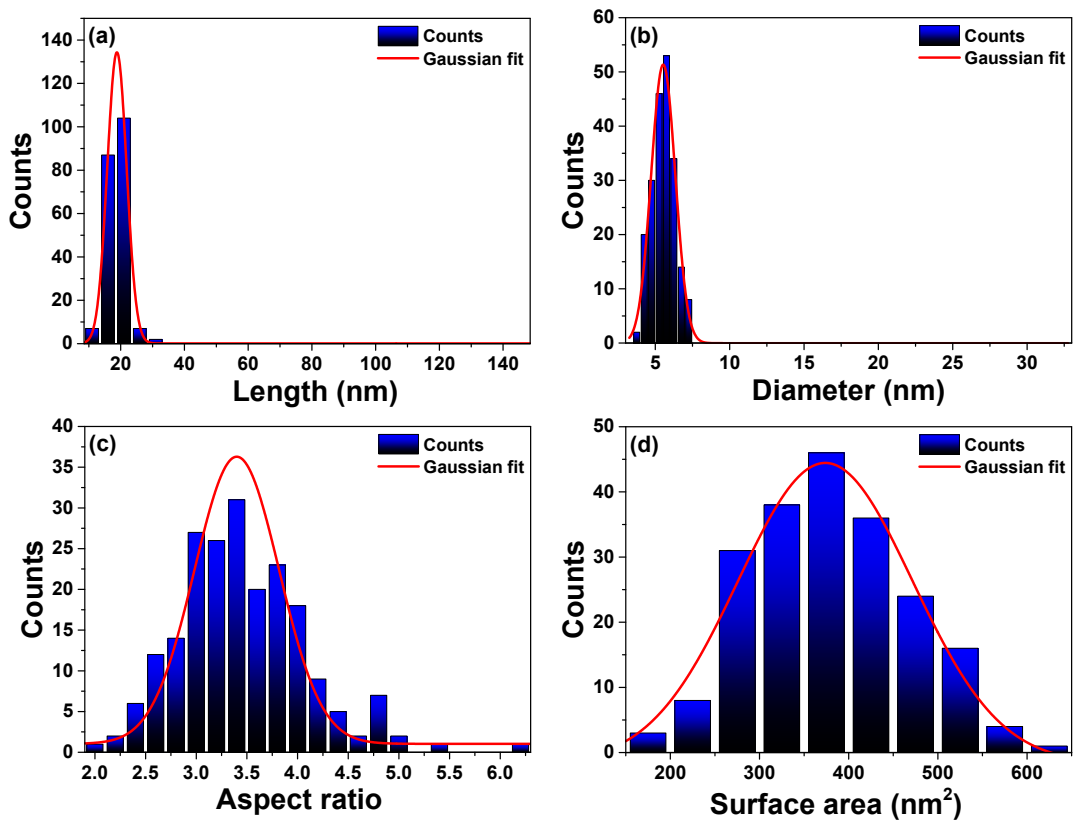

Figure S1. Dimensional distribution of NR1 (a) length (b) diameter (c) aspect ratio and (d) surface area.

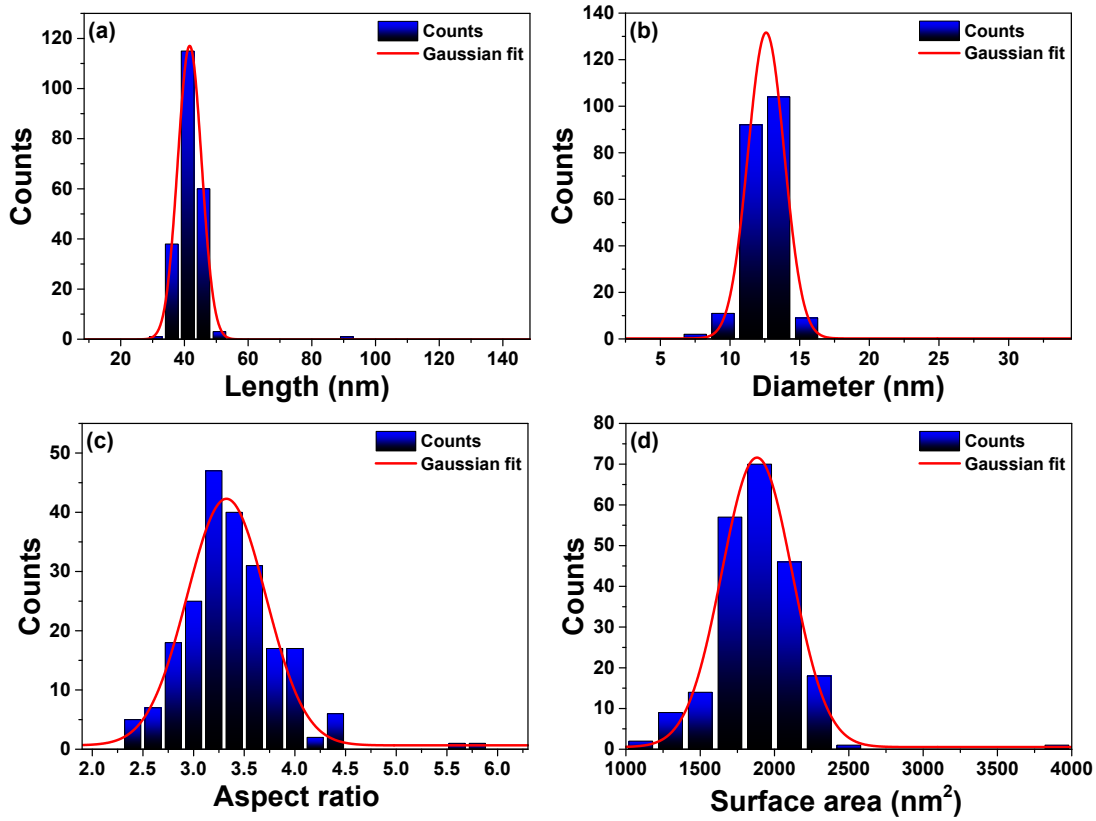

Figure S2. Dimensional distribution of NR2 (a) length (b) diameter (c) aspect ratio and (d) surface area.

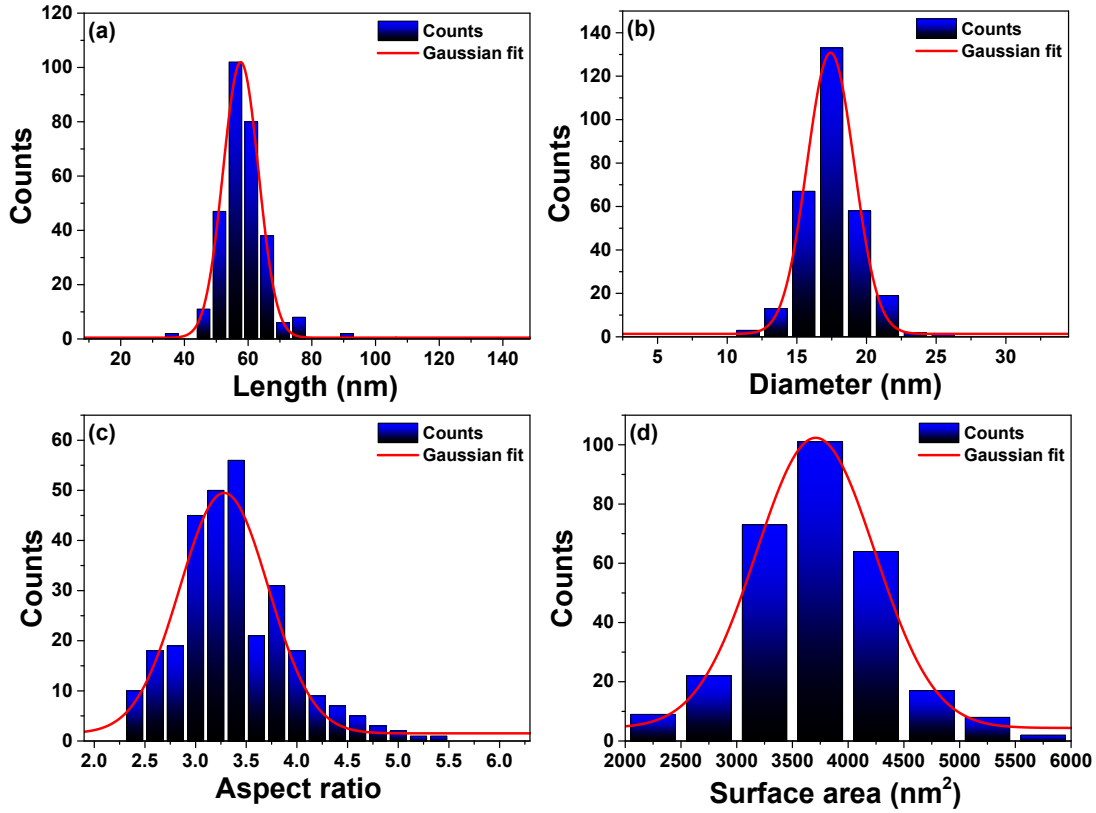

Figure S3. Dimensional distribution of NR3 (a) length (b) diameter (c) aspect ratio and (d) surface area.

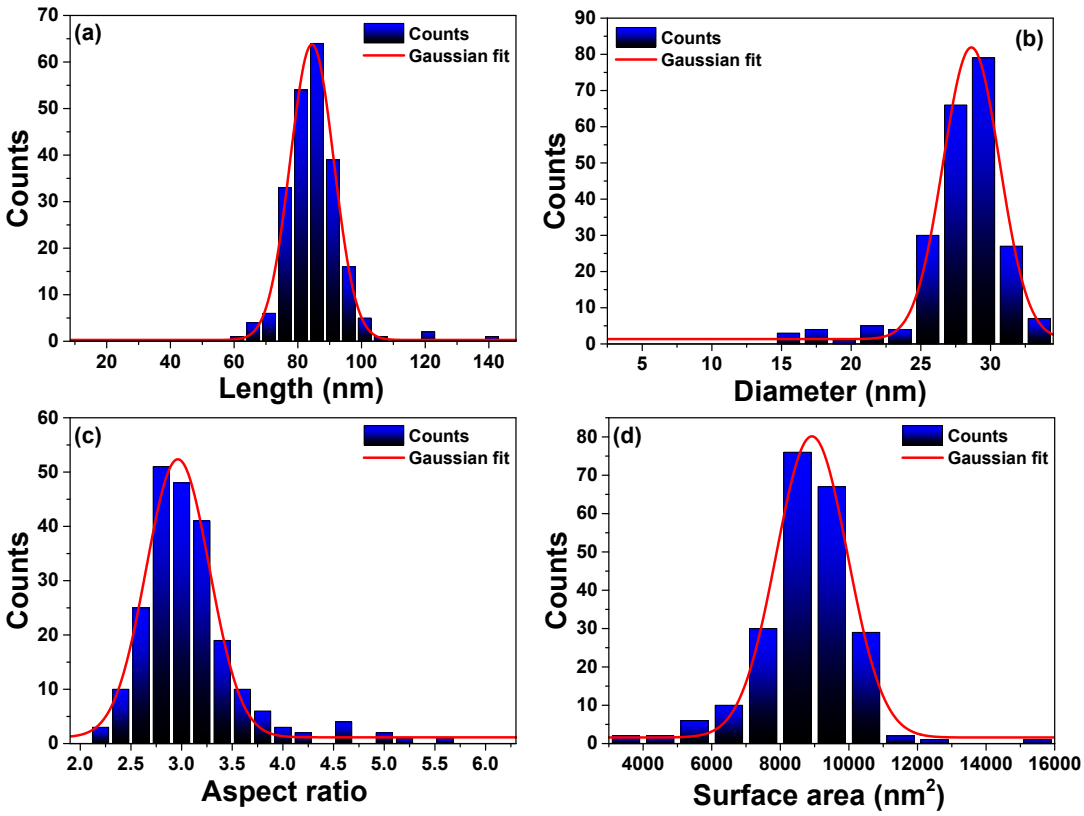

Figure S4. Dimensional distribution of NR4 (a) length (b) diameter (c) aspect ratio and (d) surface area.

3. Sample preparation protocol for surrounding refractive index (RI) modulation

The surrounding refractive index is varied using solutions of different percentages of glucose in water. A 50% glucose stock is prepared by dissolving 12 gm. of glucose in 24 mL of HPLC grade water. Eight different aliquots of 2 mL (final volume) are prepared by adding different amount of glucose stock in water in order to reach a final concentration of 0%, 10%, 15%, 20%, 25%, 30%, 35% and 40%. In the resulting solutions, gold nanorod colloid is added such that the final concentration of gold nanorods become 7.2 x 10^{-9} M (for NR1) ,1.28 x 10^{-10} M (for NR2), 5.90 x 10^{-11} M (for NR3), 1.98 x 10^{-11} M (for NR4) and 4.78 x 10^{-11} M (for NR5). For both linear and nonlinear experiments, sample preparation remains the same.

4. Variation of LSPR maxima as a function of surrounding RI

After introducing the nanorod suspension to glucose solution of different concentrations, the rods remain stable and exhibit a redshift of LSPR maxima, as expected.

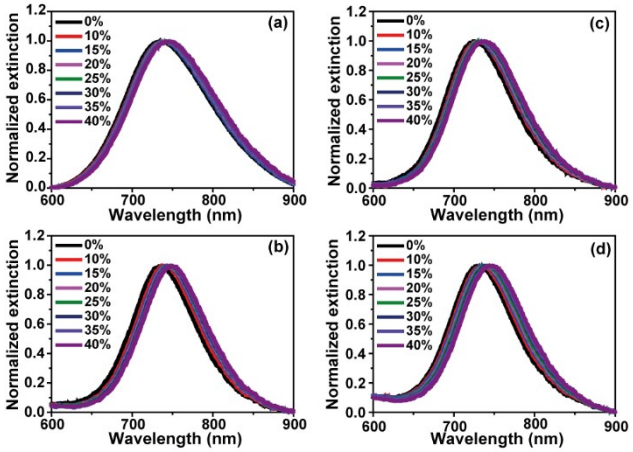

Figure 5. UV-Vis spectrum showing the variation of LSPR maxima in glucose solutions of varying concentrations for (a) NR1 (b) NR2 (c) NR3 (d) NR4.

5. Second-hamronic light scattering (SHLS) experiments

To verify the occurrence of the second-order process, we have performed two-step verification. Figure S6(a) shows the spectra of the collected signal with an excitation at 800 nm a Lorentzian peak appearing at ~ 400 nm infers a second harmonic process. In addition to this, figure S6(b) depicts a log-log plot showing the variation of the collected signal as a function of the power of the incident beam. A slope ~2 confirms the occurrence of a frequency doubling phenomenon.

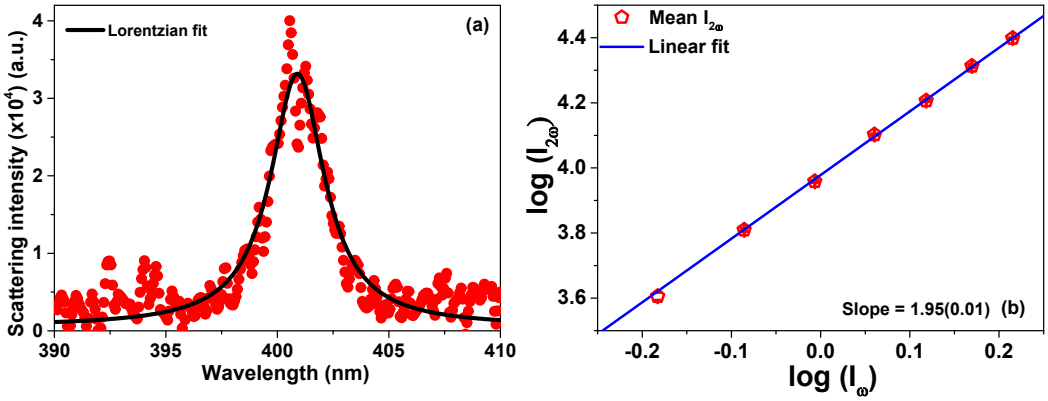

Figure S6. (a) SHLS spectra collected with an excitation wavelength of 800 nm. (b) log-log plot showing the variation of the collected signal as a function of incident power. A slope of ~2 confirms the second harmonic generation.

The following figures show the change of the normalized SHLS signal as a function of the surrounding refractive index. Each signal is divided by the number of particles present in the solution and plotted in fig. 3 of the main manuscript.

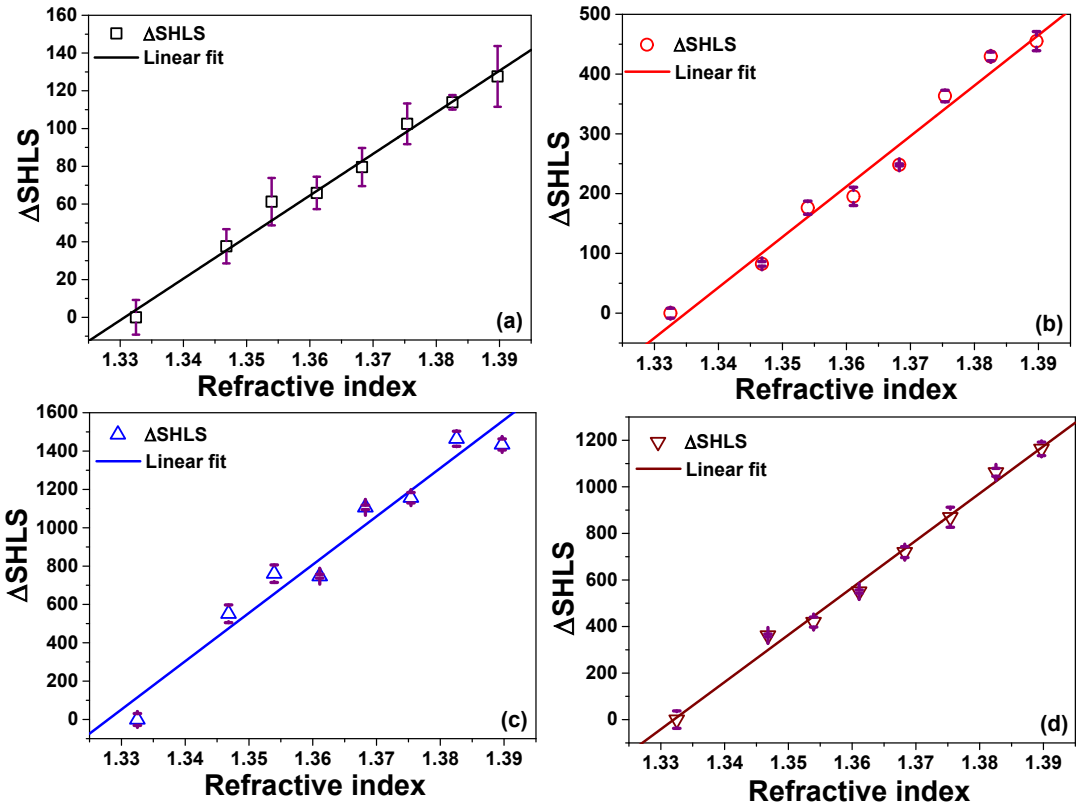

Figure S7. Variation of normalized second harmonic signal ($I_{2\omega}/I_{\omega}^2$) as a function of surrounding refractive index for (a) NR1 (b) NR2 (c) NR3 (d) NR4.

6. Three-dimensional numerical simulations

We have used a commercially available software package from Lumerical™, "FDTD solutions v8.12", to perform three-dimensional numerical simulations based on finite difference time domain technique. The details of the technique and the software can be found elsewhere[S4, S5, S6]. Briefly, the simulation setup consists of a total field scattered field (TFSF) source and 1 nm x 1 nm x 1 nm cubic mesh having a mesh accuracy of 5 around the nanostructure. The direction of propagation of the incident light is set perpendicular to the long axis of the nanorod with a polarization direction parallel to the long axis. The refractive index of the surrounding medium is varied to mimic the refractive index imparted by glucose solutions of varying concentrations. The dielectric constants for gold were obtained from the reported data of Johnson and Christy[S7]. The dimensions of nanorods used in the simulations were taken from the statistical average dimensions as determined from the electron micrograph analyses.

The nonlinear simulations were performed in a similar fashion except for some mandatory changes, the details are mentioned elsewhere[S6]. The amplitude of plane wave excitation (800 nm) was set at 1×10^8 V m^{-1}, which is fairly large than the linear source (1 V m^{-1}). A built-in time monitor is used to

provide the second harmonic response. We set the value of second-order susceptibility of gold as $\chi^{(2)} = 3 \times 10^{-10}$ mV^{-1}.

Following figure depicts the calculated SHG spectra and variation in SHG intensity as function of RI.

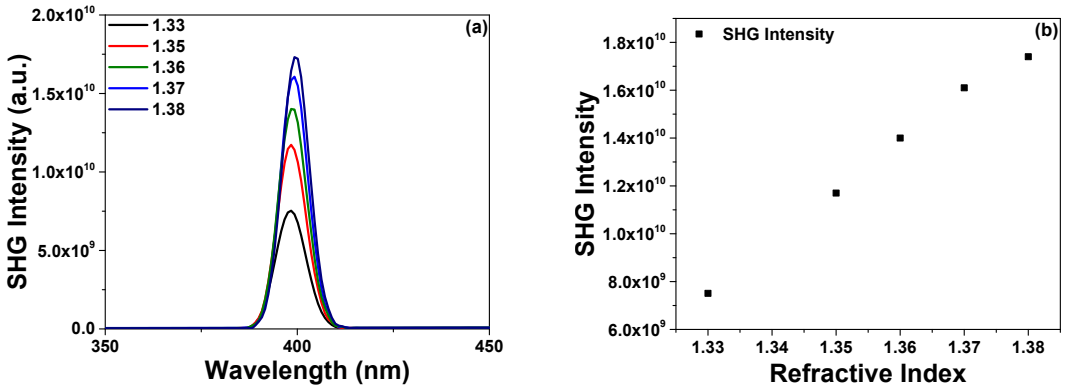

Figure S8. (a) Simulated SHG spectra at different RI and (b) variation of simulated SHG intensity as a function of RI for NR4

In the following figure electric field distribution of NR4 at 800 nm is depicted. The four different image plots are for different refractive indices.

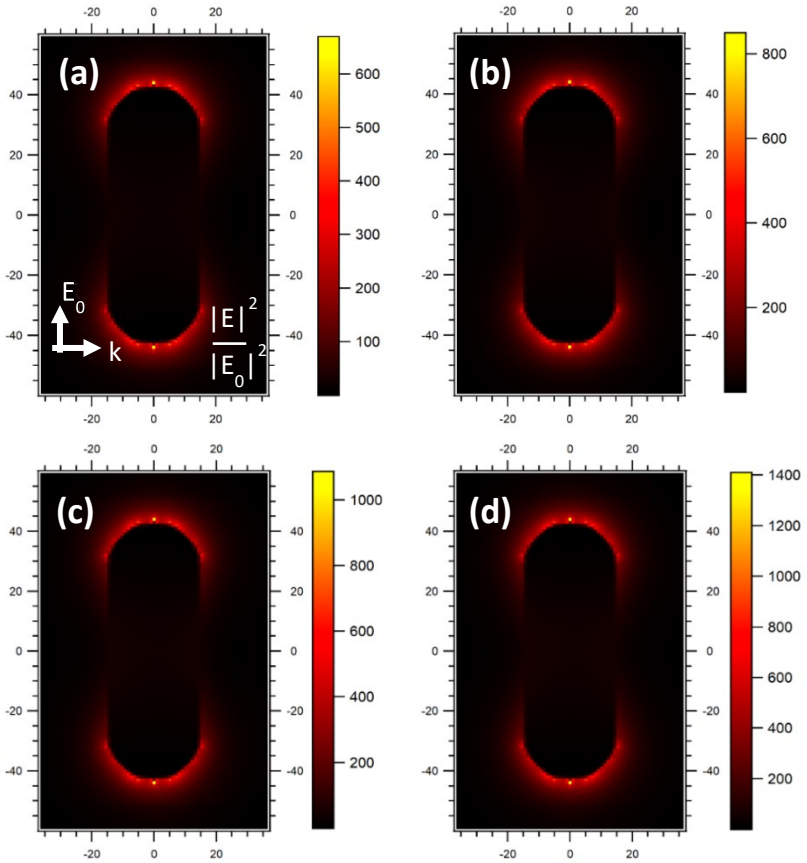

Figure S9. Numerically simulated electric field distribution of NR4 at refractive index value of (a) 1.33 (b) 1.35 (c) 1.37 (d) 1.39.

Following figure comapres the electric field distribution of NR3 and NR4 at two different refractive indices.

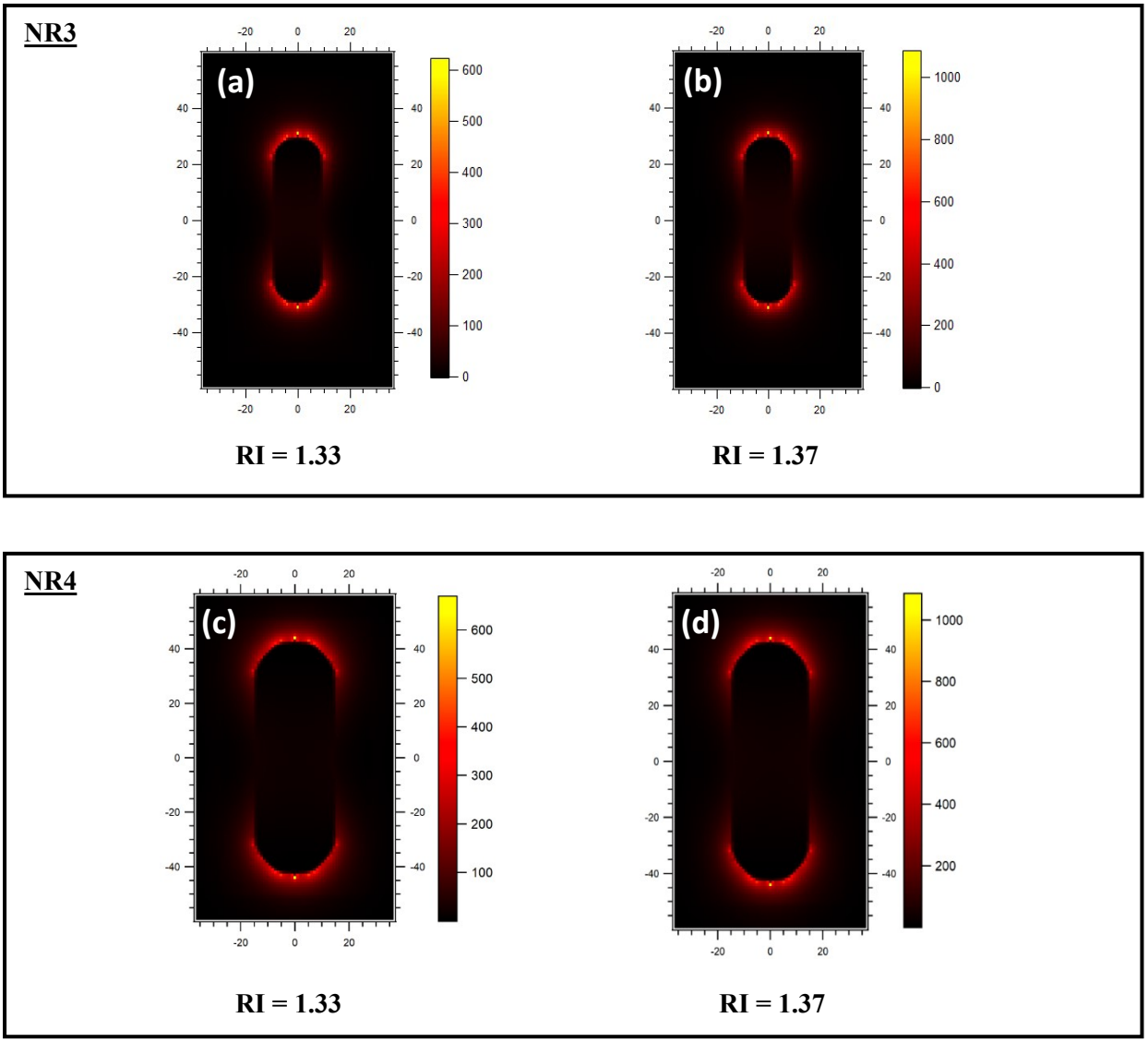

Figure S10. Numerically simulated electric field distributions of NR3 (a,b) and NR4 (c,d) at two different refractive indices.

7. Nonlinear plasmonic refractive index sensitivity of NR5

Fig. S11 shows UV-Vis spectra and representative electron micrograph for NR5. A systematic analysis of multiple images like S11(b) is done to acquire the dimensional parameters of NR5, which are summarized in Table S1.

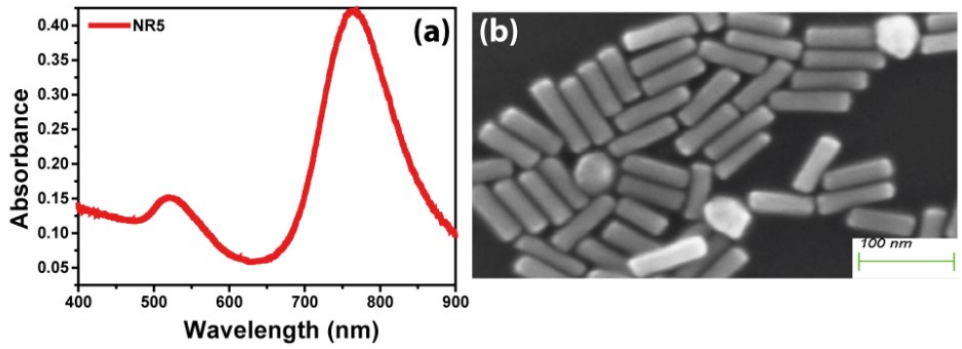

Figure S11. (a)UV-Vis extinction spectra of NR5 and (b)corresponding SEM image.

Table S1: Dimensional parameters, LSPR maximum, and nonlinear RI sensitivity of NR5.

Sample	Length (nm)	Diameter (nm)	Aspect Ratio	λ_{max} (nm)	Surface area (nm^2)	$Sensitivity_{SHLS}$ (Counts RIU^{-1})
NR5	70.30 ± 8.56	19.10 ± 2.33	3.74 ± 0.69	765	4795.58 ± 815.21	$7.71X10^{-7} \pm 2.70X10^{-8}$

Nonlinear plasmonic refractive index sensitivity for NR5 is determined in the same way as done in case of other nanorods and depicted in table S1. Fig. S12 depicts the comparison between variation in resonance enhancement contribution and actual variation of SHLS signal as a function of surrounding refractive index for NR4 and NR5. From fig. S12 (a), it is evident that the resonance enhancement increases more rapidly for NR5 than NR4 with surrounding RI. Interestingly, the second harmonic signal for NR4 increases steeply than NR5 as the RI increases. These observations confirm the role of size in determining the nonlinear plasmonic RI sensitivity of gold nanorods. Note that the data points shown in Fig. S12 are normalized to their minimum value.

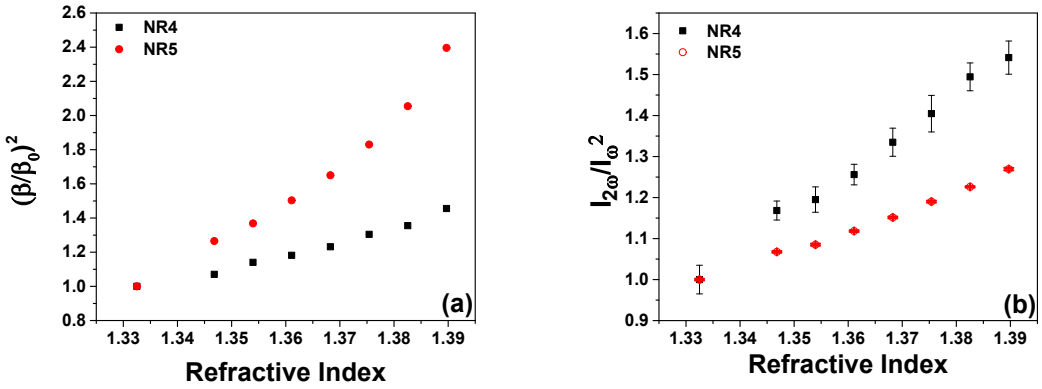

Figure S12. (a) comparison of $(\beta/\beta_0)^2$ as a function of RI for NR4 and NR5 (b) comparison of $(I_{2\omega}/I_{\omega}^2)$ as a function of RI for NR4 and NR5; the corresponding slopes are indicative of their RI sensitivities.

8. References

S1. H. H. Chang and C. J. Murphy, *Chem. Mater.*, 2018, **30**, 1427-1435.

S2. B. Nikoobakht and M. A. El-Sayed, *Chem. Mater.*, 2003, **15**, 1957-1962.

S3. L. M. Zhang, K. Xia, Z. X. Lu, G. P. Li, J. Chen, Y. Deng, S. Li, F. M. Zhou and N. Y. He, *Chem. Mater.*, 2014, **26**, 1794-1798.

S4. M. S. Verma, M. Kumar and M. Chandra, *Chem. Phys. Lett.*, 2020, **741,** 137112.

S5. B. Hazra and M. Chandra, *ACS Sens.*, 2016, **1**, 536-542.

S6. B. Hazra, K. Das and M. Chandra, *Phys. Chem. Chem. Phys.*, 2017, **19**, 18394-18399.

S7. P. B. Johnson, R. W. Christy, *Phys. Rev. B: Solid State*, 1972, **6**, 4370-4379.